Desalination 404 (2017) 72–78

Contents lists available at ScienceDirect

Desalination

journal homepage: www.elsevier.com/locate/desal

Integration of renewable energy based multigeneration system with desalination

Muhammad Shuja Azhar *, Ghaus Rizvi, Ibrahim Dincer

Faculty of Engineering and Applied Science, University of Ontario Institute of Technology, 2000 Simcoe Street North, Oshawa, Ontario L1H 7K4, Canada

HIGHLIGHTS

- New integrated multi-generation system using renewable energies is proposed.
- Integrated system is designed to heating, space cooling, electrical power and fresh water.
- Energy and exergy efficiencies of the overall system and its subsystems are calculated.

ARTICLE INFO

Article history:
Received 10 April 2016
Received in revised form 19 September 2016
Accepted 30 September 2016
Available online 10 November 2016

Keywords:
Desalination
Solar
Geothermal
OTEC
Multi-stage flash desalination
Energy
Exergy
Efficiency

ABSTRACT

The present paper comprises of an integrated system in which industrial heating, space cooling, electrical power and fresh water are produced by multigeneration system using solar, geothermal and ocean thermal energy inputs. Fresh water is produced using a multi stage flash desalination (MSF), and the direct steam generator (DSG) is used to produce power from solar. The geothermal system, with double stage flashing, is incorporated to assist solar due to its intermittent nature. The ocean thermal energy conversion (OTEC) is interconnected with desalination system while producing 30.49 kW with 0.73% energy efficiency. The proposed system is analyzed energetically and exegetically, and it is found that the energy and exergy efficiencies of the overall system are 13.93% and 17.97% respectively.

1. Introduction

Our planet has been facing pollution problems due to excessive use of fossil fuels. Power generation and transportation applications have been contributing to make our environment worse. That is why the need for clean and renewable energies has significantly increased. The main source of renewable energy for this planet is sun. Almost 170,000 TW of solar radiation falls on the Earth each year [1]. This energy from the sun is stored in earth's crust which is known as geothermal energy. Ninety nine percent of earth's volume has temperature more than 1000 °C [2]. Similarly, this energy from sun is collected by sea water. Ocean Thermal Energy Conversion (OTEC) systems are developed to harvest this energy to convert it into useful work.

Fossil fuel degradation, pollution issues and increasing oil prices are diverting attention towards renewable energy resources. Many studies are conducted on the combination of renewable resources to eliminate fossil fuel consumption. Solar energy is not enough for power production throughout a day. That is why more sources are merged to overcome this problem. The previous studies show production of multiple outputs from one system improves overall efficiency of plant [3–7]. Ozturk and Dincer [3] studied a system in which power, heat, hot water, cooling and hydrogen are produced using energy input. They combined organic Rankine, Rankine, absorption and hydrogen cycles in one system. Their obtained exergy efficiency was higher than the sub-systems efficiencies. Sinan and Dincer [4] proposed multigeneration system to produce hydrogen, electricity, heating and cooling using wind and solar energy inputs. They found that the overall efficiency of the system was higher than the individual systems. Khalid et al. [5] studied a multigeneration system with two renewable energy resources to produce multiple outputs. The calculated energy and exergy efficiencies for overall system were found higher than the efficiencies of biomass and solar systems. Suleman et al. [6] investigated a multigeneration system with solar and geothermal energy inputs to produce multiple outputs. Their study showed the advantage of using multigeneration

* Corresponding author.
E-mail addresses: shujaazhar04@gmail.com (M.S. Azhar), ghaus.rizvi@uoit.ca (G. Rizvi), ibrahim.dincer@uoit.ca (I. Dincer).

http://dx.doi.org/10.1016/j.desal.2016.09.034
0011-9164/

system over single separate energy systems. Yang et al. [7] combined ground source heat pump with fuel cell and determined that less energy consumption by hybrid system than ground source system. This shows that multigeneration systems are advantageous and gaining popularity throughout the world [8–9].

On the basis of above studies, a system is proposed with renewable resources to produce fresh water, electricity, industrial heating and space cooling. Geothermal and OTEC systems are added to assist solar energy input. No heat transfer fluid (HTF) is used in solar collectors as direct steam generation (DSG) has higher cycle temperature and thermal efficiency than indirect steam generation systems [10]. Addition of HTF will make cycle more complicated, and the efficiency will drop down. DSG plants produce 11% cheaper electricity than conventional oil heating systems [11]. To enhance power input, geothermal double flash system is incorporated in the system. Double flash geothermal can generate 20–25% more power than single flash cycle [12–14]. Around 25% of world's geothermal energy systems are based on double flash system [15].

Production of fresh water by desalinating sea water is adopted by several countries specifically in countries which have water shortage. Almost 80 countries in the world face the scarcity of fresh water [13]. Note that worldwide 27% desalination plants are thermally driven [16]. MSF plant operates at relatively lower temperature (under 100 °C) [17]. Multi-Stage flash desalination system consists of several stages. In each following stage, pressure is kept lower than the previous stage to flash the steam. In this paper MSF with three stages are selected. It is running with the combination of both solar and geothermal energy.

OTEC is a technique to harvest tidal heat energy. It is basically the temperature difference in water column of sea at different depths which could be up to 5 °C, [18] and standard depth difference is usually 1000 m [19]. The idea of OTEC, to generate electricity, was first proposed by D'Arsenoval in 1881 [20] and this concept is sometimes considered as virtually free of environmental impacts [21]. Vapor absorption cycle is interconnected with MSF plant to produce air conditioning. Coefficient of performance for single effect absorption cycle typically varies from 0.7 to 1.2 for refrigeration temperatures above 0 °C [22].

The specific objective of this study is to design and analyze thermodynamically of a new multigeneration system with solar, geothermal and OTEC energy inputs to produce fresh water, electricity, industrial heating and space cooling; and to study the effects of varying operating conditions and system parameters on the overall system performance. The calculations of energy and exergy efficiencies of the present multigeneration system and its subsystems are included in this study.

2. System description and assumptions

Solar, geothermal and OTEC sources are utilized as energy inputs while electricity, fresh water, industrial heating and space cooling are produced as the useful outputs. This system is a combination of steam turbines, pumps, generator, condenser, heat exchangers, solar collectors, mixing chamber, desalination plant, expansion valves, steam separator and cooling tower. Schematic diagram of the said system is presented in Fig. 1. All components work simultaneously to produce desired outputs using clean energy resources. The sea water entering the OTEC system is utilized in desalination plant, saving extra pump work to extract water for desalination plant. The steam injected by low pressure turbine is driving MSF plant and remaining heat is utilized by vapor absorption cycle. As this steam is the sum, of both geothermal and solar system fluids, it splits into two sections after condenser. The extra condensate is drained back to geothermal well while remaining liquid is sent back to solar field to regain energy from sun. The geothermal system is extracting saturated water at high temperature and pressure, which is being converted into steam by flashing it twice in separators A and B. The unconverted liquid drains back to the well. Following assumptions are made in analyzing the system

- The ambient temperature and pressure are assumed to be $T_o = 25$ °C and pressure $P_o = 1$ bar.
- The OTEC cycle has ammonia as the working fluid.
- The salinity of sea water for desalination plant is taken = 48,000 ppm.
- All processes are in steady state with negligible potential and kinetic energy.
- The multi-stage desalinations has three stages.
- The salt, water and saline water are incompressible substances.
- The temperature of sun is assumed to be 6000 K.

3. Thermodynamic modelling

The proposed system is analyzed both energetically and exergetically by assuming appropriate temperatures and pressures at all state points. The exergy balance equations of each component are written to find exergy destructions. Similarly efficiencies of each system, OTEC, geothermal, MSF, are calculated separately based on proposed data. Both energetic and exergetic COPs for vapor absorption cycle are determined. In the end, the overall system is assessed, and the study graphs are plotted to analyze the variation of certain parameters with respect to others. The calculations, by assuming appropriate temperature pressures at all state points, are made using Engineering Equation Solver (EES). Energy efficiencies are defined as the ratio of useful energy output to energy input [3]. The energy input from the sun is calculated as

$$\dot{Q}_{solar} = \dot{m}_1 h_1 - \dot{m}_{11} h_{11} \tag{1}$$

The solar cycle is driving turbine-A and supplying heat for industrial use. The energy and exergy efficiencies of solar cycle are defined as

$$\eta_{en,solar} = \frac{\dot{W}_{turbineA} - \dot{W}_{pump1}}{\dot{m}_1 h_1 - \dot{m}_{11} h_{11}} \tag{2}$$

$$\eta_{ex,solar} = \frac{\dot{W}_{turbineA} - \dot{W}_{pump1}}{\dot{Q}_{solar} * \left(1 - \frac{(T_o + 273)}{6000}\right)} \tag{3}$$

where

$$\dot{W}_{turbineA} = \dot{m}_1 h_1 + \dot{m}_3 h_3 - \dot{m}_2 h_2 \tag{4}$$

$$\dot{W}_{pump1} = \dot{m}_{11} h_{11} - \dot{m}_{12} h_{12} \tag{5}$$

For geothermal system, turbine B is producing output. Even more steam is injected from solar cycle as well. The efficiencies for geothermal cycle are defined as

$$\eta_{en,geo} = \frac{\dot{W}_{turbineB}}{(\dot{m}_8 h_8 - \dot{m}_{13} h_{13}) + (\dot{m}_2 h_2 - \dot{m}_5 h_5)} \tag{6}$$

$$\eta_{ex,geo} = \frac{\dot{W}_{turbineB}}{(\dot{m}_8 ex_8 - \dot{m}_{13} ex_{13}) + (\dot{m}_2 ex_2 - \dot{m}_5 ex_5)} \tag{7}$$

where

$$\dot{W}_{turbineB} = \dot{m}_5 h_5 + \dot{m}_6 h_6 - \dot{m}_{19} h_{19} \tag{8}$$

$$ex = h - h_0 - T_0(s - s_0) \tag{9}$$

$(\dot{m}_8 h_8 - \dot{m}_{13} h_{13})$ is the amount of heat extracted from geothermal source.

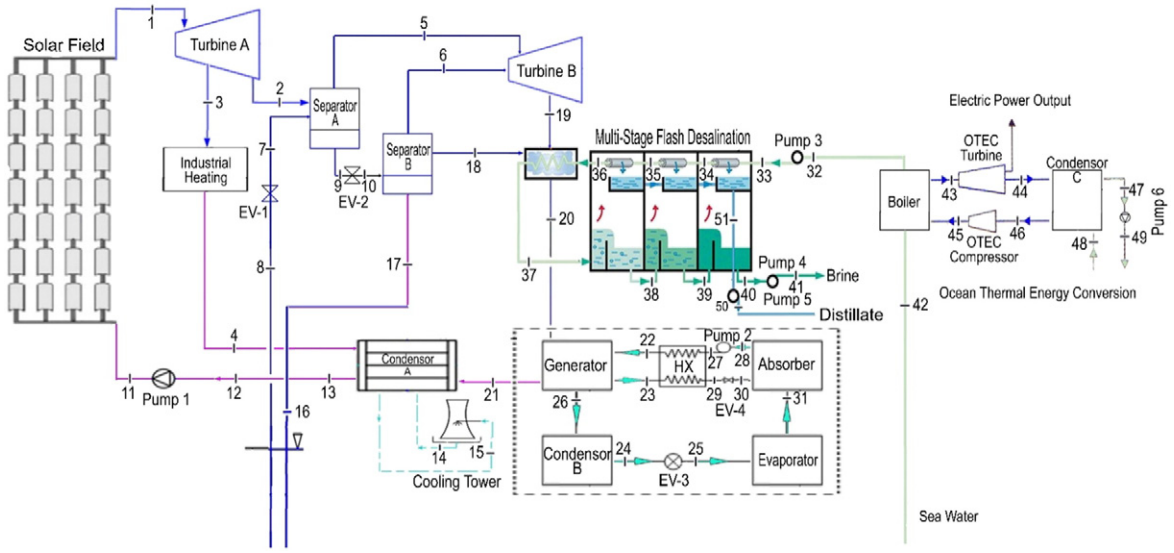

Fig. 1. Schematic diagram of multigeneration system.

The working fluid in OTEC cycle is ammonia, its boiler is getting heat energy from sea water. Its efficiencies are calculated as

$$\eta_{en,\mathrm{OTEC}} = \frac{\dot{W}_{\mathrm{OTEC}} - \dot{W}_{com\mathrm{OTEC}}}{\dot{m}_{42}h_{42} - \dot{m}_{32}h_{32}} \tag{10}$$

$$\eta_{en,\mathrm{OTEC}} = \frac{\dot{W}_{\mathrm{OTEC}} - \dot{W}_{com\mathrm{OTEC}}}{\dot{m}_{42}ex_{42} - \dot{m}_{32}ex_{32}} \tag{11}$$

where the work output produced by OTEC turbine is

$$\dot{W}_{\mathrm{turbineOTEC}} = \dot{m}_{43}h_{43} + \dot{m}_{44}h_{44} \tag{12}$$

And the work consumed by OTEC compressor is

$$\dot{W}_{\mathrm{comOTEC}} = \dot{m}_{45}h_{45} + \dot{m}_{46}h_{46} \tag{13}$$

The desalination efficiency is defined dividing difference of brine, fresh and sea water with energy input into the heating chamber of desalination plant. Both energy and exergy efficiencies are then written as

$$\eta_{en,des} = \frac{\dot{m}_{41}h_{41} + \dot{m}_{50}h_{50} - \dot{m}_{32}h_{32}}{\dot{m}_{19}h_{19} - \dot{m}_{20}h_{20}} \tag{14}$$

$$\eta_{ex,des} = \frac{\dot{m}_{41}ex_{41} + \dot{m}_{50}ex_{50} - \dot{m}_{32}ex_{32}}{\dot{m}_{19}ex_{19} - \dot{m}_{20}ex_{20}} \tag{15}$$

Both energetic and exegetic COPs for the absorption cycle are calculated as

$$\mathrm{COP}_{en} = \frac{\dot{m}_{25}h_{25} - \dot{m}_{31}h_{31}}{\dot{m}_{20}h_{20} - \dot{m}_{21}h_{21}} \tag{16}$$

$$\mathrm{COP}_{ex} = \frac{\dot{m}_{25}ex_{25} - \dot{m}_{31}ex_{31}}{\dot{m}_{20}ex_{20} - \dot{m}_{21}ex_{21}} \tag{17}$$

The network produced by the system can be find by Eq. (18) while other pump works can be calculated using energy balance equations given in Table 1

$$\dot{W}_{net} = \dot{W}_{\mathrm{turbineA}} + \dot{W}_{\mathrm{turbineB}} + \dot{W}_{\mathrm{turbineOTEC}} - \dot{W}_{com\mathrm{OTEC}} - \dot{W}_{\mathrm{pump1}} - \dot{W}_{\mathrm{pump2}} - \dot{W}_{\mathrm{pump3}} - \dot{W}_{\mathrm{pump4}} - \dot{W}_{\mathrm{pump5}} - \dot{W}_{\mathrm{pump6}} \tag{18}$$

For overall energy efficiency, other output entities are formulated as

$$\dot{Q}_{\mathrm{cooling}} = \dot{m}_{25}h_{25} - \dot{m}_{31}h_{31} \tag{19}$$

$$\dot{Q}_{\mathrm{desalination}} = \dot{m}_{41}h_{41} + \dot{m}_{50}h_{50} - \dot{m}_{32}h_{32} \tag{20}$$

$$\dot{Q}_{\mathrm{heating}} = (\dot{m}_{3}h_{3} - \dot{m}_{4}h_{4}) \tag{21}$$

$$\dot{Q}_{\mathrm{geothermal}} = \dot{m}_{8}h_{8} - \dot{m}_{13}h_{13} \tag{22}$$

$$\dot{Q}_{\mathrm{OTEC}} = (\dot{m}_{42}h_{42} - \dot{m}_{32}h_{32}) \tag{23}$$

The total energy input from solar, geothermal and OTEC energy sources are

$$\dot{Q}_{\mathrm{total}} = \dot{Q}_{\mathrm{solar}} + \dot{Q}_{geo} + \dot{Q}_{\mathrm{OTEC}} \tag{24}$$

The overall energy efficiency for the whole system is determined as

$$\eta_{en,ov} = \frac{\dot{W}_{net} + \dot{Q}_{\mathrm{cooling}} + \dot{Q}_{\mathrm{desalination}} + \dot{Q}_{\mathrm{heating}}}{\dot{Q}_{\mathrm{total}}} \tag{25}$$

Similarly, all above entities are formulated to find the overall exergy of the system

$$Ex._{\mathrm{cooling}}^{\mathrm{Q}} = \dot{m}_{25}ex_{25} - \dot{m}_{31}ex_{31} \tag{26}$$

$$Ex._{\mathrm{desalination}}^{\mathrm{Q}} = \dot{m}_{41}ex_{41} + \dot{m}_{50}ex_{50} - \dot{m}_{32}ex_{32} \tag{27}$$

$$Ex._{\mathrm{heating}}^{\mathrm{Q}} = (\dot{m}_{3}ex_{3} - \dot{m}_{4}ex_{4}) \tag{28}$$

$$Ex._{geo}^{\mathrm{Q}} = \dot{m}_{8}ex_{8} - \dot{m}_{13}ex_{13} \tag{29}$$

$$Ex._{\mathrm{OTEC}}^{\mathrm{Q}} = (\dot{m}_{42}ex_{42} - \dot{m}_{32}ex_{32}) \tag{30}$$

$$Ex._{\mathrm{solar}}^{\mathrm{Q}} = \dot{Q}_{\mathrm{solar}} * \left(1 - \frac{(T_o + 273)}{6000}\right) \tag{31}$$

Table 1

Name of the component	Energy equations	Exergy equations
Solar Collector	$\dot{m}_1 h_1 = \dot{Q}_{in,solar} + \dot{m}_{11} h_{11}$	$\dot{m}_1 ex_1 + \dot{E}_x \dot{Q}_{in,solar} = \dot{m}_{11} ex_{11} + \dot{E}x_{dsolar}$
Turbine – A	$\dot{m}_1 h_1 = \dot{m}_2 h_2 + \dot{m}_3 h_3 + \dot{W}_{turbine_A}$	$\dot{m}_1 ex_1 = \dot{m}_2 ex_2 + \dot{m}_3 ex_3 + \dot{W}_{turbine_A} + \dot{E}x_{dturbineA}$
Turbine – B	$\dot{m}_5 h_5 + \dot{m}_6 h_6 = \dot{m}_{19} h_{19} + \dot{W}_{turbine_B}$	$\dot{m}_5 ex_5 + \dot{m}_6 ex_6 = \dot{m}_{19} ex_{19} + \dot{W}_{turbine_B} + \dot{E}x_{dturbineB}$
OTEC Turbine	$\dot{m}_{43} h_{43} = \dot{m}_{44} h_{44} + \dot{W}_{OTEC}$	$\dot{m}_{43} ex_{43} = \dot{m}_{44} ex_{44} + \dot{W}_{OTEC} + \dot{E}x_{dturbineOTEC}$
OTEC Compressor	$\dot{m}_{46} h_{46} + \dot{W}_{comOTEC} = \dot{m}_{45} h_{45}$	$\dot{m}_{46} ex_{46} + \dot{W}_{comOTEC} = \dot{m}_{45} ex_{45} + \dot{E}x_{dcomOTEC}$
OTEC Boiler	$\dot{m}_{42} h_{42} + \dot{Q}_{in,OTEC} = \dot{m}_{43} h_{43}$	$\dot{m}_{42} ex_{42} + \dot{E}_x \dot{Q}_{in,OTEC} = \dot{m}_{43} ex_{43} + \dot{E}x_{dboiler}$
Pump - 1	$\dot{m}_{12} h_{12} + \dot{W}_{pump_1} = \dot{m}_{11} h_{11}$	$\dot{m}_{12} ex_{12} + \dot{W}_{pump_1} = \dot{m}_{11} ex_{11} + \dot{E}x_{d_{pump1}}$
Pump – 2	$\dot{m}_{28} h_{28} + \dot{W}_{pump_2} = \dot{m}_{27} h_{27}$	$\dot{m}_{28} ex_{28} + \dot{W}pump2 = \dot{m}_{27} ex_{27} + \dot{E}x_{dpump2}$
Pump – 3	$\dot{m}_{32} h_{32} + \dot{W}_{pump_3} = \dot{m}_{33} h_{33}$	$\dot{m}_{32} ex_{32} + \dot{W}_{pump_3} = \dot{m}_{33} ex_{33} + \dot{E}x_{d_{pump3}}$
Pump – 4	$\dot{m}_{41} h_{41} + \dot{W}_{pump4} = \dot{m}_{40} h_{40}$	$\dot{m}_{41} ex_{41} + \dot{W}_{pump_4} = \dot{m}_{40} ex_{40} + \dot{E}x_{d_{pump4}}$
Pump – 5	$\dot{m}_{50} h_{50} + W_{pump_5} = \dot{m}_{54} h_{54}$	$\dot{m}_{50} ex_{50} + \dot{W}_{pump_5} = \dot{m}_{54} ex_{54} + \dot{E}x_{d_{pump5}}$
Pump – 6	$\dot{m}_{49} h_{49} + \dot{W}_{pump_6} = \dot{m}_{47} h_{47}$	$\dot{m}_{49} ex_{49} + \dot{W}_{pump6} = \dot{m}_{47} ex_{47} + \dot{E}x_{dpump6}$
Separator – A	$\dot{m}_7 h_7 = \dot{m}_{18} h_{18} + \dot{m}_9 h_9$	$\dot{m}_7 ex_7 = \dot{m}_{18} ex_{18} + \dot{m}_9 ex_9 + \dot{E}x_{d_{sepA}}$
Separator – B	$\dot{m}_{10} h_{10} = \dot{m}_6 h_6 + \dot{m}_{17} h_{17}$	$\dot{m}_{10} ex_{10} = \dot{m}_6 ex_6 + \dot{m}_{17} ex_{17} + \dot{E}x_{d_{sepB}}$
Condenser – A	$\dot{m}_4 h_4 + \dot{m}_{14} h_{14} + \dot{m}_{21} h_{21} = \dot{m}_{13} h_{13} + \dot{m}_{15} h_{15}$	$\dot{m}_4 ex_4 + \dot{m}_{14} ex_{14} + \dot{m}_{21} ex_{21} = \dot{m}_{13} ex_{13} + \dot{m}_{15} ex_{15} + \dot{E}x_{d_{conA}}$
Condenser – B	$\dot{m}_{26} h_{26} = \dot{m}_{24} h_{24}$	$\dot{m}_{26} ex_{26} = \dot{m}_{24} ex_{24} + \dot{E}x_{d_{conB}}$
Condenser – C	$\dot{m}_{44} h_{44} + \dot{m}_{48} h_{48} = \dot{m}_{46} h_{46} + \dot{m}_{47} h_{47}$	$\dot{m}_{44} ex_{44} + \dot{m}_{48} ex_{48} = \dot{m}_{46} ex_{46} + \dot{m}_{47} ex_{47} + \dot{E}x_{d_{conC}}$
Generator	$\dot{m}_{20} h_{20} + \dot{m}_{22} h_{22} = \dot{m}_{21} h_{21} + \dot{m}_{23} h_{23} + \dot{m}_{26} h_{26}$	$\dot{m}_{20} ex_{20} + \dot{m}_{22} ex_{22} = \dot{m}_{21} ex_{21} + \dot{m}_{23} ex_{23} + \dot{m}_{26} ex_{26} + \dot{E}x_{d_x} + \dot{E}x_{d_{gen}}$
Absorber	$\dot{m}_{28} h_{28} = \dot{m}_{30} h_{30} + \dot{m}_{31} h_{31}$	$\dot{m}_{28} ex_{28} = \dot{m}_{30} ex_{30} + \dot{m}_{31} ex_{31} + \dot{E}x_{d_{abs}}$
Evaporator	$\dot{m}_{25} h_{25} = \dot{m}_{31} h_{31}$	$\dot{m}_{25} ex_{25} = \dot{m}_{31} ex_{31} + \dot{E}x_{d_{evap}}$
Expansion Valve – 1	$\dot{m}_7 h_7 = \dot{m}_8 h_8$	$\dot{m}_7 ex_7 = \dot{m}_8 ex_8 + \dot{E}x_{d_{ev1}}$
Expansion Valve – 2	$\dot{m}_9 h_9 = \dot{m}_{10} h_{10}$	$\dot{m}_9 ex_9 = \dot{m}_{10} ex_{10} + \dot{E}x_{dev2}$
Expansion Valve – 3	$\dot{m}_{24} h_{24} = \dot{m}_{25} h_{25}$	$\dot{m}_{24} ex_{24} = \dot{m}_{25} ex_{25} + \dot{E}x_{d_{ev3}}$
Expansion Valve – 4	$\dot{m}_{29} h_{29} = \dot{m}_{30} h_{30}$	$\dot{m}_{29} ex_{29} = \dot{m}_{30} ex_{30} + \dot{E}x_{d_{ev4}}$
Cooling Tower	$\dot{m}_{15} h_{15} = \dot{m}_{14} h_{14} + \dot{Q}_{loss}$	$\dot{m}_{15} ex_{15} = \dot{m}_{14} ex_{14} + \dot{E}x_{d_{ct}} + \dot{E}x^{Q}_{loss}$
Heat Exchanger	$\dot{m}_{27} h_{27} + \dot{m}_{23} h_{23} = \dot{m}_{22} h_{22} + \dot{m}_{29} h_{29}$	$\dot{m}_{27} ex_{27} + \dot{m}_{23} ex_{23} = \dot{m}_{22} ex_{22} + \dot{m}_{29} ex_{29} + \dot{E}x_{d_{hx}}$
Industrial Heating	$\dot{m}_3 h_3 = \dot{m}_4 h_4 + \dot{Q}_{heating}$	$\dot{m}_3 ex_3 = \dot{m}_4 ex_4 + \dot{E}x_{d_{heating}} + \dot{E}x^{Q}_{heating}$
Mixing Chamber	$\dot{m}_2 h_2 + \dot{m}_{18} h_{18} = \dot{m}_5 h_5$	$\dot{m}_2 ex_2 + \dot{m}_{18} ex_{18} = \dot{m}_5 ex_5 + \dot{E}x_{d_{mc}}$

The total exergy input is the sum of individual exergy input from heat energy sources

$$Ex\cdot^{Q}_{total} = Ex\cdot^{Q}_{solar} + Ex\cdot^{Q}_{geo} + Ex\cdot^{Q}_{OTEC} \tag{32}$$

The overall exergy efficiency is defined thermodynamically as

$$\eta_{ex,ov} = \frac{\dot{W}_{net} + Ex\cdot^{Q}_{heating} + Ex\cdot^{Q}_{cooling} + Ex\cdot^{Q}_{desalination}}{Ex\cdot^{Q}_{total}} \tag{33}$$

4. Results and discussion

The specific enthalpy, entropy and exergy at each point are calculated as tabulated in Table 2, while the flowrates are set by iteration to get optimum performance. Fig. 2 shows exergy destructions of main components of the proposed system. The highest exergy destruction is found in concentrated solar collectors which is much higher than any other component. Turbine B and mixing chamber has second and third highest exergy destructions. Special attention needs to be paid in reducing the exergy destruction rate for solar collectors to improve overall efficiency of the system. Table 3 summarizes all the results generated from calculation work including cooling and heating loads, energy and exergy efficiencies of each system, overall energy and exergy efficiency, power outputs, collector area, solar irradiation and COPs of absorption cycle.

Fig. 3 shows the effects of exit temperature (T_1) from DSG on solar cycle efficiencies and overall system efficiencies. Being the main working fluid for the whole system, energy and exergy efficiencies are increasing with the increase in temperature. But to get higher temperature and more energy input, area of collector needs to be expanded. Higher temperature and high energy content will increase power production. On the other hand, if HTF is introduced, then heat exchanger addition will cause heat energy to lose causing drop in overall efficiency.

Fig. 4 shows the relation of solar irradiation on the solar and overall efficiencies. No effect is been observed on solar cycle, energy and exergy efficiencies, by varying solar irradiation, from 400 W/m^2 to 800 W/m^2, while there is slight increase in overall energy efficiency i.e. from 13.3% to 14.3%. The reason of no effect, on solar efficiencies, is the direct link of power output of turbine A with incoming fluid, means higher the solar radiations higher will be the power output. Hence, solar efficiencies will remain unaffected by irradiations while overall efficiencies will ramp up. Irradiation will increase power output, but in comparison to overall system, its effect is minimal.

Fig. 5 is illustrated based on the study of relation between mass flowrate extracted from geothermal well on geothermal cycle and overall cycle efficiency. Both efficiencies are dropping down by the increment of flowrate ($\dot{m}_8$) from 250 kg/s to 350 kg/s. The overall efficiency is dropping from 6.47% to 5.56%. Note that it makes no sense to pull more fluid as it will depict inverse effect on the whole system. The quality of saturated water from well is not sufficient to surge efficiency. More than half of the incoming fluid, that does not flash into steam, goes back to the well without being used in any process. So increase in $\dot{m}_8$ will reduce $\dot{m}_1$ causing overall as well as geothermal efficiency to drop.

Similarly, the output temperature of the geothermal well, T_8, has exactly the same effect as of $\dot{m}_8$. Even trends in Fig. 6 look much similar to Fig. 5. Thus, the reason is obviously the same for temperature as well. The steam from solar cycle is being injected into geothermal mixing chamber. If mass $\dot{m}_1$ increases then ultimately flowrate from geothermal well has to be decreased in order to manage the flowrate entering turbine B which will cause drop in geothermal efficiency.

The energy and exergy efficiencies of desalination plant have direct relation with mass flowrate coming in from the sea. Fig. 7 shows straight

Table 2
Calculated thermodynamic values.

State point	Temperature [°C]	Pressure (bar)	Mass flowrate [kg/s]	Specific enthalpy [kJ/kg]	Specific entropy [kJ/kgK]	Specific exergy [kJ/kg]	Salinity (g/kg)
1	380	50	200	3146	6.57	1192	–
2	217.4	20	100	2813	6.37	919.8	–
3	335	25	100	3091	6.783	1074	–
4	110	1	100	2696	7.415	491.1	–
5	214.7	20	212.7	2806	6.354	916.7	–
6	179.9	10	9.933	2778	6.586	819.6	–
7	212.4	20	250	1761	4.202	513.2	–
8	360	24	250	1761	3.915	598.7	–
9	212.4	20	137.3	908.7	2.447	183.9	–
10	179.9	10	137.3	908.7	2.461	179.9	–
11	98.82	50	200	417.8	1.29	37.94	–
12	99.63	1	200	417.5	1.303	33.8	–
13	99.63	1	322.7	417.5	1.303	33.8	–
14	22	1	2	92.29	0.3246	0.057	–
15	26	1	2	109	0.3809	0.009	–
16	38	1	250	159.2	0.5454	1.179	–
17	100	1	127.3	2676	7.361	486.8	–
18	212.4	20	112.7	2799	6.34	914	–
19	120.2	2	222.7	2707	7.127	587.1	–
20	99.63	1	222.7	2449	6.753	441.4	–
21	85	–	222.7	1963	5.621	292.3	–
22	340	10	164.3	641.7	2.492	220.7	–
23	348	10	118.3	467.4	1.986	481.6	–
24	305	10	46	1245	4.206	313.2	–
25	270	3	46	1206	4.582	161.7	–
26	358	10	46	1460	4.861	117.1	–
27	323.7	10	164.3	366.5	1.665	191.7	–
28	292	3	164.3	364.9	1.833	140.2	–
29	310	3	118.3	349.7	1.788	138.5	–
30	295	1	118.3	450.8	2.298	87.6	–
31	290	3	46	1292	4.892	155.9	–
32	25	1	200	97.79	0.3391	0.035	–
33	25.1	5	200	98.18	0.3404	0.039	48
34	40	5	200	156.9	0.5325	2.007	48
35	70	5	200	275.7	0.8948	13.91	48
36	90	5	200	355	1.12	26.88	48
37	110	5	200	434	1.332	43.36	48
38	96.71	0.9	197.5	381.3	1.191	32.02	48
39	85.95	0.6	195.6	338.5	1.073	23.93	48.62
40	60.07	0.2	188.4	235.4	0.7743	8.872	49.08
41	60.17	1	188.4	235.8	0.7755	8.917	50.96
42	28	1	200	109.6	0.3785	0.194	50.96
43	20	6.9	1.914	1494	5.519	271.9	48
44	11.9	–	1.914	1478	5.519	255.9	–
45	–	6.9	1.914	262.2	1.221	321	–
46	11.9	–	1.914	255.3	1.197	321.2	–
47	8	1	185.9	33.71	0.1213	2.072	–
48	5	1	185.9	21.12	0.07625	2.898	–
49	8.2	1	185.9	34.54	0.1242	2.022	–
50	60.17	1	18.54	251.9	0.8333	13.4	–
51	96.71	0.9	2.547	405.2	1.27	37.82	0
52	85.95	0.6	4.387	359.9	1.145	29.24	0
53	60.07	0.2	11.61	251.5	0.8321	13.35	0
54	60.07	0.2	11.61	251.5	0.8321	13.35	0

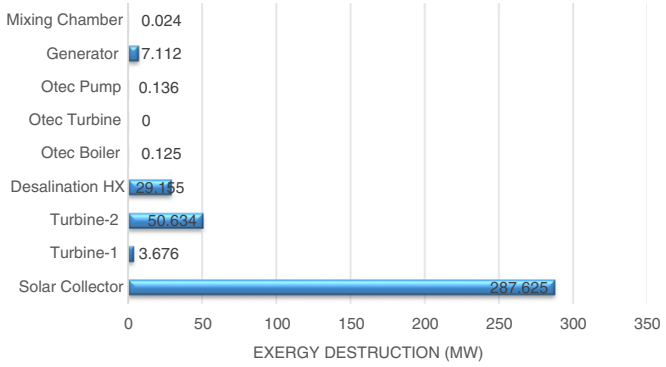

Fig. 2. Exergy destructions of major components.

Table 3
Values of parameters obtained from modelling.

Description	Value	Unit
Work turbine-A	33.209	MW
Work turbine-B	21.785	MW
Solar collector area	909,261	m^2
Solar irradiation	600	W/m^2
Solar energy efficiency	13.93	%
Solar exergy efficiency	7.44	%
Geothermal energy efficiency	6.47	%
Geothermal exergy efficiency	15.39	%
Industrial heating	39.48	MW
Salinity of sea water	48,000	ppm
Fresh water production	18.54	kg/s
MSF Energy efficiency	51.58	%
MSF Exergy efficiency	5.92	%
W_{OTEC}	30.49	kW
OTEC energy efficiency	0.73	%
OTEC exergy efficiency	54.58	%
Cooling load	3.98	MW
COP energetic	0.03674	–
COP exergetic	0.007978	–
Overall energy efficiency	13.93	%
Overall exergy efficiency	17.97	%

direct relation on $\dot{m}_{42}$. Increasing flowrate from 200 kg/s to 300 kg/s, energy efficiency is ramping up from 51.58% to 77.36%. But the point is, energy input should also be increased correspondingly to manage the same effect on efficiency. Otherwise it looks obvious, more sea water input, more will be the product of fresh water. In order to maintain MSF plant efficiency, both flowrates $\dot{m}_1$ and $\dot{m}_{42}$ needs to be increased proportionally to produce more or less fresh water output. Altering both flowrates is not easy at once, as other subsystems may drastically be affected by this change. MSF plant is connected with OTEC cycle in a way that incoming water is providing heat to the boiler of OTEC system. Means only one pump is enough for both the system, saving extra pump work for OTEC cycle.

The energetic and exergetic COPs have direct relation with temperature of saturated water exiting from generator of absorption cycle. Fig. 8 shows clear illustration of the said statement, means higher the exit temperature (T_{21}), higher will be the COP. The variation of energetic COP is observed changing from 0.03499 to 0.03647 while increasing the temperature from 75 °C to 85 °C. It all depends on the energy content available in the incoming fluid. If the fluid entering generator has higher temperature, it should then be released at higher temperature while transferring energy to absorption cycle. The overall exergy efficiency will remain unchanged by varying temperature T_{21}.

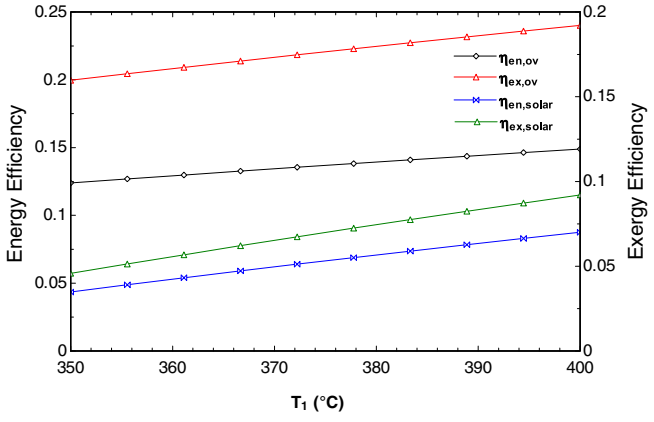

Fig. 3. Effect of temperature (T_1) on energy and exergy efficiencies of solar system and overall system.

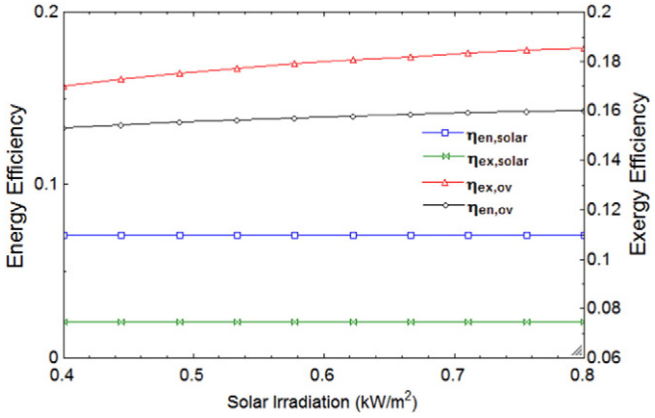

Fig. 4. Effect of solar irradiation on energy and exergy efficiencies of solar system and overall system.

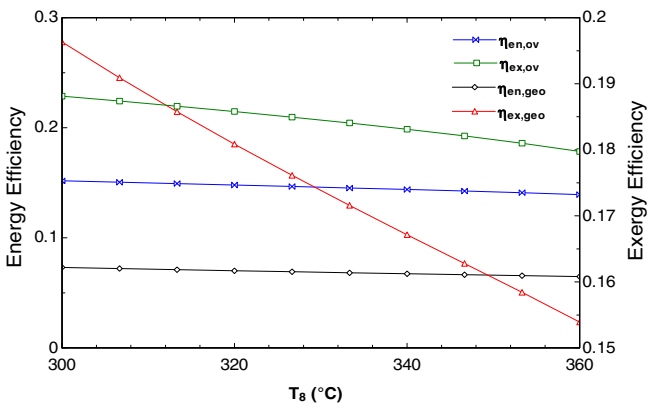

Fig. 6. Effect of temperature (T_8) on energy and exergy efficiencies of geothermal system and overall system.

The effect of ambient temperature is analyzed both on overall energy and exergy efficiencies. Fig. 9 shows exergy efficiency is directly proportional to ambient temperature. Changing ambient temperature from 15 °C to 25 °C the exergy efficiency increases from 17.66% to 17.97%. This rise in exergy efficiency is minimal or may be negligible to observe the effect of varying ambient temperature on the overall system performance. Energy efficiency has no effect of ambient temperature. This cycle can be operated in normal environmental temperature of 15 °C to 25 °C with no effect in efficiency.

Numerous studies have already been conducted on multigeneration systems for thermodynamic assessment. This design appears to be different from others in a sense that OTEC is introduced with other renewable systems. Although its performance becomes low, it still offers a good opportunity for improvement and hence better performance.

5. Conclusions

A new multigeneration system with solar, geothermal and OTEC energy inputs, to produce electricity, industrial heating, space cooling and fresh water, is designed and assessed using energy and exergy analyses and efficiency assessments. The exergy destructions of major components are calculated. The solar collector has the highest exergy destruction of 287.62 MW while desalination HX and turbine-2 are two other components with high exergy destruction. Thus, the efforts need to be made to minimize these exergy destructions for the better performance of the system. The area of solar collector required is found to be 909,261 m^2 while the total power output is almost 55 MW. Geothermal and solar options are the main sources of energy, which produce 18.54 kg/s of fresh water by MSF distillation plant with 51.58% energy efficiency, and providing industrial heating up to 39.48 MW. Similarly, energetic COP is found to be 0.03674. OTEC is producing 30.49 kW with efficiency of 0.73%. Furthermore it is found that the overall energy and exergy efficiencies of the system are 13.93% and 17.97% respectively.

Nomenclature

ex	specific exergy (kJ/kg)
$\dot{E}x$	exergy rate (kW)
h	specific enthalpy (kJ/kg)
$\dot{m}$	mass flow rate (kg/s)
P	pressure (kPa)
$\dot{Q}$	heat transfer rate (kW)
s	specific entropy (kJ/kgK)
T	temperature (°C)
$\dot{W}$	work rate (kW)

Greek letters

η	efficiency

Subscript

abs	absorber
com	compressor
con	condenser
ct	cooling tower
d	destruction
des	desalination
en	energy
ev	expansion valve
evap	evaporator
ex	exergy

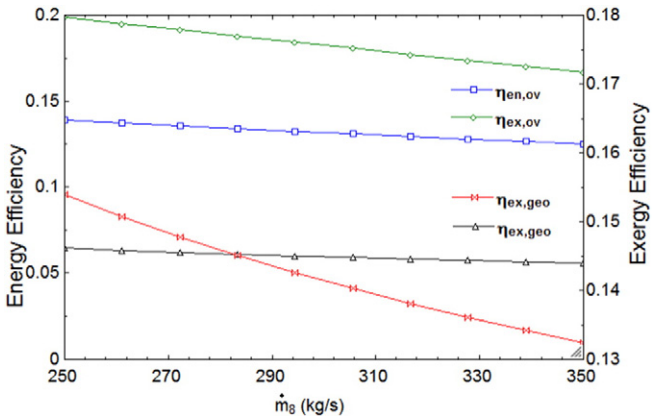

Fig. 5. Effect of mass flowrate ($\dot{m}_8$) on energy and exergy efficiencies of geothermal system and overall system.

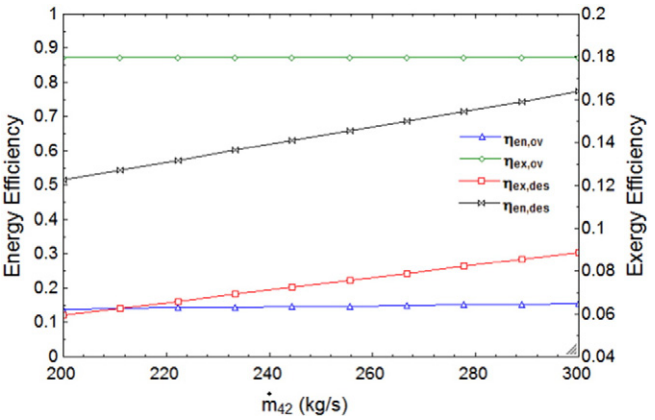

Fig. 7. Effect of mass flowrate ($\dot{m}_{42}$) on overall efficiency of the system and desalination plant efficiencies of the system.

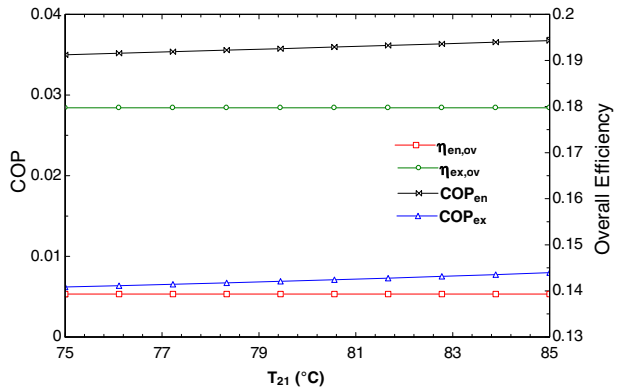

Fig. 8. Effect of the exit temperature of the absorption cycle (T_{21}) on COP and overall efficiencies of the system.

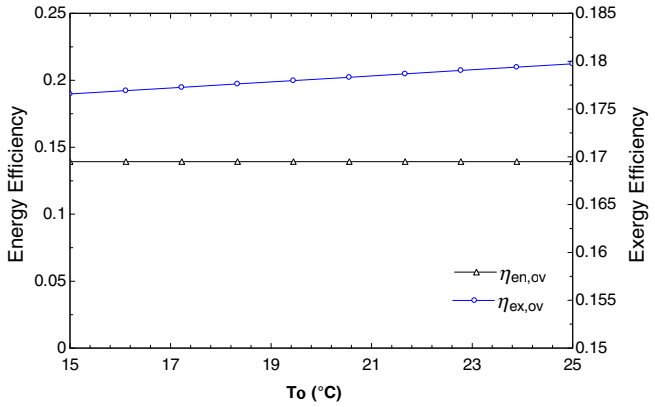

Fig. 9. Effect of ambient temperature (T_0) on overall energy and exergy efficiencies of the system.

gen	generator
geo	geothermal
hx	heat exchanger
mc	mixing chamber
OTEC	ocean thermal energy
ov	overall
sep	separator
1, 2, …	state numbers
Acronyms	
COP	Coefficient of Performance
DSG	Direct Steam Generator
EV	Expansion Valve
HTF	Heat Transfer Fluid
HX	Heat Exchanger
MED	Multi Effect Desalination
MSF	Multi Stage Flash Distillation
OTEC	Ocean Thermal Energy Conversion

References

[1] A. Etemadi, A. Emdadi, O. AsefAfshar, Y. Emami, Electricity generation by the ocean thermal energy, Energy Procedia 12 (2011) 936–943.
[2] P. Bayer, L. Rybach, P. Blum, R. Brauchler, Review on life cycle environmental effecs of geothermal power generation, Renew. Sust. Energ. Rev. 46 (2013) 446–463.
[3] M. Ozturk, I. Dincer, Thermodynamic analysis of a solar-based multigeneration system with hydrogen production, Appl. Therm. Eng. 51 (2013) 1235–1244.
[4] S. Ozlu, I. Dincer, Development and analysis of a solar and wind energy based multigeneration system, Sol. Energy 122 (2015) 1279–1295.
[5] F. Khalid, I. Dincer, M.A. Rosen, Energy and exergy analyses of a solar-biomass integrated cycle for multigeneration, Sol. Energy 112 (2015) 290–299.
[6] F. Suleman, I. Dincer, M. Agelin-Chaab, Development of an integrated renewable energy system for multigeneration, Energy 78 (2014) 196–204.
[7] L. Yang, E. Entchev, M. Ghorab, E.J. Lee, E.C. Kang, Energy and cost analyses of a hybrid renewable microgeneration system serving multiple residential and small office buildings, Appl. Therm. Eng. 65 (2014) 477–486.
[8] A.S. Sánchez, E.A. Torres, R.A. Kalid, Renewable energy generation for the rural electrification of isolated communities in the Amazon Region, Renew. Sust. Energ. Rev. 49 (2015) 278–290.
[9] P. De Jong, A.S. Sánchez, K. Esquerre, R.A. Kalid, E.A. Torres, Solar and wind energy production in relation to the electricity load curve and hydroelectricity in the northeast region of Brazil, Renew. Sust. Energ. Rev. 23 (2013) 526–535.
[10] N. Fraidenraich, C. Oliveira, A.F. Vieira da Cunha, J.M. Gordon, O.C. Vilela, Analytical modeling of direct steam generation solar power plants, Sol. Energy 98 (2013) 511–522.
[11] J. Birnbaum, J.F. Feldhoff, M. Fichtner, T. Hirsch, M. Jocker, R. Pitz-Paal, G. Zimmermann, Steam temperature stability in a direct steam generation solar power plant, Sol. Energy 85 (2011) 660–668.
[12] A. Dagdas, Performance analysis and optimization of double-flash geothermal power plants, Journal of Energy Resources Technology 129 (2007) 125–133.
[13] J. Clarke, J.T. McLeskey Jr., The constrained design space of double-flash geothermal power plants, Geothermics 51 (2014) 31–37.
[14] J.R. Sarr, F. Mathieu-Potvin, Improvement of double-flash geothermal power plant design: q comparison of six interstage heating processes, Geothermics 54 (2015) 82–95.
[15] H. Kang, Y. Yang, Z. Chang, H. Zheng, Z. Duan, Performance of a two-stage multi-effect desalination system based on humidification–dehumidification process, Desalination 344 (2014) 339–349.
[16] M.W. Shahzad, K.C. Ng, K. Thu, B.B. Saha, W.G. Chun, Multi effect desalination and adsorption desalination (MEDAD): a hybrid desalination method, Appl. Therm. Eng. 72 (2014) 289–297.
[17] N. Kahraman, Y.A. Cengel, Exergy analysis of a MSF distillation plant, Energy Convers. Manag. 46 (2005) 2625–2636.
[18] P. Ahmadi, I. Dincer, M.A. Rosen, Performance assessment of a novel solar and ocean thermal energy conversion based multi-generation system for coastal areas, Journal of Solar Energy Engineering 137 (2015) 011013-1-12.
[19] D.E. Lennard, The viability and best conditions for ocean thermal energy conversion systems around the world, Renew. Energy 6 (1995) 359–365.
[20] R. Soto, J. Vergara, Thermal power plant efficiency enhancement with ocean thermal energy conversion, Appl. Therm. Eng. 62 (2014) 105–112.
[21] R. Fujita, A.C. Markham, J.E. Diaz, J.R.M. Garcia, C. Scarborough, P. Greenfield, P. Black, S.E. Aguilera, Revisiting ocean thermal energy conversion, Mar. Policy 36 (2012) 463–465.
[22] S. Wu, I.W. Eames, Innovations in vapour-absorption cycles, Appl. Energy 66 (2000) 251–266.